(Fig. 5C) can potentially reduce the ability of these receptors to compete with effector T cells and other immune cell types for IL-1 and IL-6, cytokines that enhance T_H17 differentiation (*3*, *10*, *23*). In this regard, IL-2 receptor expressed on T_{regs} can deprive effector T cells of IL-2, thereby, effectively limiting the immune response (*24*). Consistent with this idea, Stat3-sufficient, but not Stat3-deficient, T_{regs} depleted IL-1 and IL-6 from the culture medium (fig. S17).

Unexpectedly, Stat3 deficiency in T_{regs} resulted in increased expression of *Il6*, *Tgfb1*, and *Vip*. Although T_{reg}-produced TGF-β1 can mediate suppression (*25*), TGF-β1 in combination with IL-6 also facilitates the generation of T_H17 cells. Similarly, *Vip*-encoded vasoactive intestinal peptide (VIP) promotes T_H17 differentiation (*26*). Indeed, soluble factors produced by Stat3-deficient T_{regs} facilitated differentiation of IL-17–producing T cells in vitro in the absence of exogenously supplied IL-6 and TGF-β1 (Fig. 5F). Increased expression of IL-6 and TGF-β1 in Stat3-deficient T_{regs} (Fig. 5, B and D) might amplify, but cannot fully account for, the observed increase in IL-17 production in diseased $Foxp3^{Cre}Stat3^{fl/fl}$ mice because heterozygous $Foxp3^{Cre/wt}Stat3^{fl/fl}$ female mice cohabited by Stat3-deficient and -sufficient T_{regs} do not exhibit augmented T_H17 responses.

To test whether Stat3 facilitates recruitment of Foxp3 to regulatory elements of *Il6* and *Tgfb1* genes, we used chromatin immunoprecipitation combined with quantitative polymerase chain reaction (qPCR) to examine Foxp3 binding to promoter regions of these genes in Stat3-sufficient and -deficient T_{reg} cells. Indeed, we found that Foxp3 was bound to *Il6* and *Tgfb1* promoters in a Stat3-dependent manner. In contrast, Foxp3 binding to *Zfpn1a2* (Helios) and *Il2ra*, well-known Foxp3-binding genes expressed in a Stat3-independent manner, was unaffected by the absence of Stat3 (Fig. 5G). These results suggest that Stat3 activation–dependent association with Foxp3 transcriptional complexes may result in modulation of Stat3-dependent gene expression partly through Stat3-dependent recruitment of Foxp3.

Thus, the activation of Stat3 in T_{regs} endows them with the ability to suppress T_H17 responses plausibly through increased expression of a subset of suppressor molecules, as well as cytokine and chemokine receptors, which may deprive immune effector cells of essential activation cues and facilitate the spatial proximity of T_{regs} and T_H17 cells. Furthermore, Stat3 in T_{regs} limits the expression of soluble mediators of T_H17 differentiation. We suggest that altered expression of a combination of genes, but not changes in any one of them, can account for the inability of Stat3-deficient T_{regs} to restrain T_H17 responses.

Our findings support the idea that the same transcription factors integrate environmental cues that guide a particular immune response type and facilitate T_{reg} cells' ability to suppress the corresponding type of immune response. Consistent with this notion, Irf4 (interferon regulatory factor 4), an IRF transcription factor family member essential for T_H2 differentiation, is required for T_{reg} cells to suppress T_H2 responses (*27*). Furthermore, T_{reg} expression of T-bet, a T_H1-specific transcription factor, is required for T_{reg} homeostasis under conditions of induced T_H1 inflammation (*28*). We propose that the STAT-IRF axis of transcriptional regulation allows T_{regs} to adapt to a particular environment and ensures appropriate "class"-specific control of immune-mediated inflammation.

References and Notes

1. P. R. Mangan *et al.*, *Nature* **441**, 231 (2006).
2. M. Veldhoen, R. J. Hocking, C. J. Atkins, R. M. Locksley, B. Stockinger, *Immunity* **24**, 179 (2006).
3. L. Zhou *et al.*, *Nat. Immunol.* **8**, 967 (2007).
4. X. O. Yang *et al.*, *Immunity* **28**, 29 (2008).
5. E. Bettelli, T. Korn, M. Oukka, V. K. Kuchroo, *Nature* **453**, 1051 (2008).
6. S. Hori, T. Nomura, S. Sakaguchi, *Science* **299**, 1057 (2003).
7. J. D. Fontenot, M. A. Gavin, A. Y. Rudensky, *Nat. Immunol.* **4**, 330 (2003).
8. I. I. Ivanov *et al.*, *Cell* **126**, 1121 (2006).
9. E. Bettelli *et al.*, *Nature* **441**, 235 (2006).
10. L. Zhou *et al.*, *Nature* **453**, 236 (2008).
11. T. Korn *et al.*, *Nature* **448**, 484 (2007).
12. Y. P. Rubtsov *et al.*, *Immunity* **28**, 546 (2008).
13. J. M. Kim, J. P. Rasmussen, A. Y. Rudensky, *Nat. Immunol.* **8**, 191 (2007).
14. W. Strober, I. J. Fuss, R. S. Blumberg, *Annu. Rev. Immunol.* **20**, 495 (2002).
15. K. J. Maloy, M. C. Kullberg, *Mucosal Immunol.* **1**, 339 (2008).
16. I. I. Ivanov *et al.*, *Cell Host Microbe* **4**, 337 (2008).
17. S. A. Khader *et al.*, *Nat. Immunol.* **8**, 369 (2007).
18. A. Reboldi *et al.*, *Nat. Immunol.* **10**, 514 (2009).
19. M. A. Gavin *et al.*, *Nature* **445**, 771 (2007).
20. D. A. Vignali, L. W. Collison, C. J. Workman, *Nat. Rev. Immunol.* **8**, 523 (2008).
21. M. Kleinewietfeld *et al.*, *Blood* **105**, 2877 (2005).
22. T. Yamazaki *et al.*, *J. Immunol.* **181**, 8391 (2008).
23. C. Sutton, C. Brereton, B. Keogh, K. H. Mills, E. C. Lavelle, *J. Exp. Med.* **203**, 1685 (2006).
24. P. Pandiyan, L. Zheng, S. Ishihara, J. Reed, M. J. Lenardo, *Nat. Immunol.* **8**, 1353 (2007).
25. M. O. Li, Y. Y. Wan, R. A. Flavell, *Immunity* **26**, 579 (2007).
26. M. Yadav, J. Rosenbaum, E. J. Goetzl, *J. Immunol.* **180**, 2772 (2008).
27. Y. Zheng *et al.*, *Nature* **458**, 351 (2009).
28. M. A. Koch *et al.*, *Nat. Immunol.* **10**, 595 (2009).

29. We thank K. Forbush, T. Chu, L. Karpik, and A. Bravo for assistance with the mouse colony management; S. Akira for *Stat3*$^{fl/fl}$ mice; and J. Renauld for antibody to IL-22. This work was supported by NIH grants AI-061816 and AI-034206. A.C. is supported by the Cancer Research Institute, and D.R. is supported by the Arthritis Foundation. A.Y.R. is an investigator with the Howard Hughes Medical Institute. Gene expression microarray data have been deposited in the NCBI Gene Expression Omnibus repository with the accession code GSE17962.

Supporting Online Material

www.sciencemag.org/cgi/content/full/1172702/DC1
Methods
Figs. S1 to S17
References

24 February 2009; accepted 2 September 2009
Published online 1 October 2009;
10.1126/science.1172702
Include this information when citing this paper.

A Spindle Assembly Checkpoint Protein Functions in Prophase I Arrest and Prometaphase Progression

Hayden Homer,* Liming Gui, John Carroll

Two critical stages of mammalian oocyte regulation are prophase I arrest, which is important for sustaining the oocyte pool, and the progression through meiosis I (MI) to produce fertilizable eggs. We have found that the spindle assembly checkpoint protein BubR1 regulates both stages in mouse oocytes. We show that oocytes depleted of BubR1 cannot sustain prophase I arrest and readily undergo germinal vesicle breakdown, a marker for reentry into MI. BubR1-depleted oocytes then arrest before completing MI, marked by failure of polar body extrusion. Both meiotic defects in BubR1-depleted oocytes are due to reduced activity of the master regulator known as the anaphase-promoting complex (APC), brought about through diminished levels of the APC coactivator Cdh1.

Mammalian oocytes arrest at prophase I from birth until puberty when hormonal signals induce the resumption of meiosis I (MI) and progression to meiosis II (MII), the stage at which fertilization occurs. Prophase I–arrested oocytes possess an intact nucleus referred to as the germinal vesicle (GV), with GV breakdown (GVBD) and first polar body extrusion (PBE) signifying the resumption and conclusion of MI, respectively (Fig. 1A). Cell-cycle progression is driven by a proteolytic machinery known as the anaphase-promoting complex (APC) acting in concert with one of two coactivators, Cdc20 or Cdh1 (*1*). Unlike mitotic prometaphase—in which APC-Cdc20 is the principal APC species (*1*)—in mammalian oocytes, APC-Cdh1 is active during prophase I (*2*, *3*) and early prometaphase I before APC-Cdc20, which acts in late MI (*4*) (Fig. 1A). In both systems, however, the anaphase-trigger is APC-Cdc20–mediated securin and cyclin B1 degradation (*1*, *4*, *5*). The key inhibitor of APC-Cdc20–dependent anaphase onset is the spindle assembly checkpoint (SAC), the core compo-

Oocyte and Embryo Research Laboratory, Department of Cell and Developmental Biology, Division of Biosciences and Institute for Women's Health, University College London, London, UK.

*To whom correspondence should be addressed. E-mail: h.homer@ucl.ac.uk

nents of which are drawn from the Mad and Bub protein families (*6*). Mitotic arrest deficient 2 (Mad2) and Bub1 have predicted APC-Cdc20–directed SAC roles in mouse oocytes and consequently regulate late MI coincident with APC-Cdc20 activity (*7*, *8*). Here, we examine the role of another key SAC protein, BubR1, in mouse oocytes where APC-Cdh1 is active before activation of APC-Cdc20.

We employed a morpholino-based gene-silencing approach (*9*) to deplete BubR1 in oocytes (*2*, *7*). Using a *BubR1*-targeting morpholino (termed BubR1MO) (*9*), we depleted ~80% of endogenous BubR1 (fig. S1). During the course of evaluating BubR1MO, we found that 25% of BubR1-depleted oocytes spontaneously underwent GVBD in 3-isobutyl-1-methylxanthine (IBMX), a drug that maintains prophase I arrest in almost 98% of control and Mad2-depleted oocytes (Fig. 1B) (*2*, *9*). This indicated that BubR1-depleted oocytes have reduced capacity for sustaining prophase I arrest. In mouse oocytes, the prophase I arrest state is dependent upon APC-Cdh1 activity (*2*, *3*). We therefore examined Cdh1 in BubR1-depleted oocytes and found that it was reduced by ~60% (Fig. 1C). This reduction in Cdh1 levels was specific to BubR1 depletion, because Cdh1 was unaffected by Mad2-depletion (Fig. 1C), and Cdh1 levels could be restored in BubR1MO-injected oocytes by coexpressing human BubR1 (hBubR1) from *hBubR1* complementary RNA (cRNA) (Fig. 1D). This suggested that the fragility of prophase I arrest after BubR1 depletion was due to reduced APC-Cdh1 activity. In support of this, GVBD rates in BubR1-depleted oocytes declined considerably after restoring Cdh1 levels by injecting either *Cdh1* cRNA or *hBubR1* cRNA (Fig. 1B). Thus, by maintaining APC-Cdh1 activity, BubR1 is important for prophase I arrest in mouse oocytes, consistent with a prophase I role for homologs of BubR1 in yeast and flies (*10*, *11*).

Although BubR1-depleted oocytes readily resumed MI, there was a marked reduction in PBE rates. By 10 hours after GVBD, 80% of control oocytes undergo PBE, contrasting sharply with only 6% of BubR1-depleted oocytes (Fig. 2, A and B). This effect was not anticipated, because BubR1, like Mad2, is known to inhibit APC-Cdc20 (*1*, *6*). Indeed, we find that in oocytes, BubR1 exhibits properties typical of an SAC protein, including the capacity for APC-Cdc20 inhibition (fig. S2). Hence, BubR1 depletion would be expected to prematurely activate APC-Cdc20 and to advance MI exit, as occurs after Mad2 depletion (Fig. 2A) (*7*). Instead, BubR1-depleted oocytes undergo an MI arrest (Fig. 2, A and B), which implies that BubR1 has additional functions during MI separate from its SAC role.

To explore the mechanism of MI arrest in BubR1-depleted oocytes, we examined the levels of securin and cyclin B1. We observed that after BubR1 depletion, securin and cyclin B1 levels remained stable by 8 hours after GVBD, whereas both proteins had been destroyed in controls (Fig. 2C and fig. S3). Given that securin and cyclin B1 destruction are required for anaphase I (*4*, *5*), this indicated that BubR1-depleted oocytes arrest before anaphase I. We confirmed this by immunostaining spindles and chromosomes. By 10 hours after GVBD and beyond, BubR1-depleted oocytes show no evidence of anaphase I, telophase I, or MII configurations, all of which are apparent in controls between 8 and 10 hours after GVBD (Fig. 2, D and E). Together, these data show that BubR1-depleted oocytes arrest in prometaphase I.

APC-Cdh1 is active during prometaphase I (Fig. 1A), the stage at which BubR1-depleted oocytes arrest. Given that we have found BubR1 to be important for Cdh1 stability in prophase I (Fig. 1, C and D), a similar BubR1-dependent effect on APC-Cdh1 in prometaphase I could plausibly underpin prometaphase I arrest after BubR1 depletion. This prompted us to examine Cdh1 levels during MI. As with prophase I, after BubR1 depletion, Cdh1 was again reduced by 50 to 70% throughout prometaphase I, whereas Cdc20 was unaffected (Fig. 3, A to C). In the reverse experiment, BubR1 overexpression stabilized Cdh1 (fig. S4, A and B). This supported our hypothesis that deregulated APC-Cdh1 is central to prometaphase I arrest after BubR1 depletion. Moreover, because Mad2 does not share BubR1's influence on Cdh1 levels (Fig. 1C), this explains why BubR1 and Mad2 depletion produce contrasting phenotypes.

We therefore focused on the first 6 hours of MI when APC-Cdh1 is active (Fig. 1A) and examined securin and cyclin B1, two recognized APC-Cdh1 substrates that must be meticulously regulated for proper M-phase progression (*1*). We observed that during early prometaphase I, securin was twice as high as in BubR1-depleted oocytes compared with controls, whereas cyclin B1 was unaffected (Fig. 3, D to F). Thus, after BubR1 depletion, Cdh1 is reduced and securin is increased. The inverse relationship between Cdh1 and securin was consistent with securin being a preferential APC-Cdh1 substrate during early prometaphase I, as is the case during prophase I (*2*) and in mitosis (*12*). In support of this, we found that securin, but not cyclin B1, was stabilized during early prometaphase I in oocytes depleted of Cdh1 (Fig. 3, D to F, fig. S5, and fig. S11). The converse was also true, because Cdh1 overexpression led to a reduction in securin (fig. S6). Hence, these data show that low-level APC-Cdh1–mediated securin destruction occurs during prometaphase I and is BubR1-dependent. As further confirmation of BubR1 dependency, we found that the extent of the Cdh1 decrease and securin increase was proportional to the severity of BubR1 depletion (fig. S7). Moreover, BubR1 overexpression increased Cdh1 and decreased securin (fig. S4, A to C), changes that were exactly opposite to those induced by BubR1 depletion. Thus, APC-Cdh1–mediated securin destruction during early prometaphase I is BubR1-dependent and is required for preventing overaccumulation of securin.

Next, we asked whether failure of anaphase I in BubR1-depleted oocytes (Fig. 2) might be attributable to high securin levels. We now turned our attention to APC-Cdc20, because anaphase I

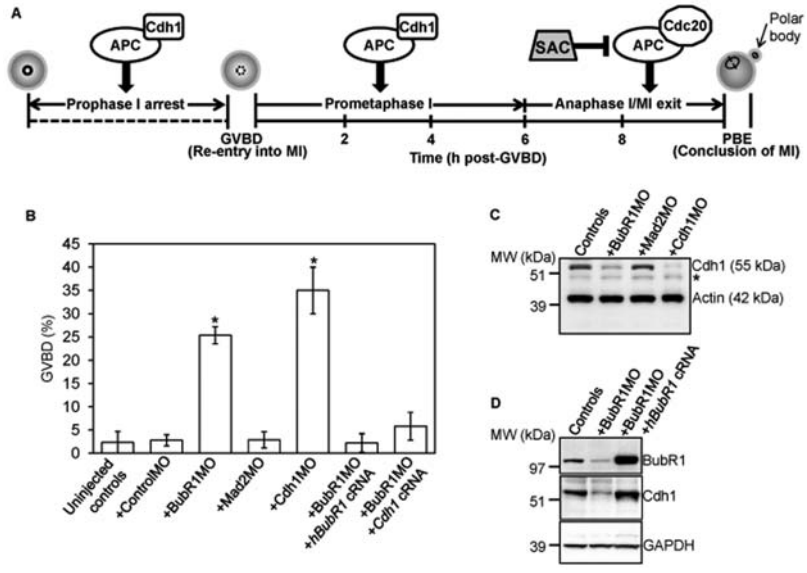

Fig. 1. Prophase I arrest is compromised after BubR1 depletion. (**A**) Schematic of MI. (**B**) Mock-depleted (+ControlMO), BubR1-depleted (+BubR1MO), Mad2-depleted (+Mad2MO) (*7*), Cdh1-depleted (+Cdh1MO), (*9*) and uninjected oocytes were scored for GVBD after 24 hours in IBMX. Cdh1-depleted oocytes escape prophase I arrest as shown previously (*2*). Increased GVBD after BubR1 depletion could be prevented by expressing either BubR1 from an *hBubR1* cRNA (+BubR1MO+*hBubR1* cRNA) or Cdh1 from a *Cdh1* cRNA (+BubR1MO+*Cdh1* cRNA) (*9*). Error bars, mean ± SEM; $N \geq 3$ experiments. Asterisks denote a significant difference from uninjected controls ($P < 0.0001$; Student's *t*-test). (**C** and **D**) Samples (50 oocytes) of GV-stage oocytes from each of the groups depicted were immunoblotted either for Cdh1 and actin (C) or for BubR1, Cdh1, and glyceraldehyde phosphate dehydrogenase (GAPDH) (D) ($N = 2$ experiments). *, Nonspecific band.

is mediated by late-acting APC-Cdc20 and not by APC-Cdh1 (*4*) (Fig. 1A). Anaphase I is vulnerable to any perturbation of the natural balance between APC-Cdc20 and either securin or cyclin B1. For instance, overexpression of securin from an exogenous *Securin-GFP* cRNA invokes a prometaphase I arrest (*5*) by overwhelming APC-Cdc20. Similarly, prometaphase I arrest after BubR1 depletion could arise if APC-Cdc20 was being outstripped by elevated securin. If this were so, one clear prediction is that redressing the presumed APC-Cdc20/securin mismatch should enable BubR1-depleted oocytes to undergo anaphase I and to exit MI. Consistent with this notion, PBE rates were significantly increased in BubR1-depleted oocytes either by overexpressing Cdc20 or by restraining securin expression (from 6% to 40% and 66%, respectively) (fig. S8).

Notably, however, PBE rates in BubR1-depleted oocytes were not fully restored to wild-type levels after reinstating a favorable APC-Cdc20/securin balance (fig. S8). This suggested that other deficits after BubR1 knockdown, such as kinetochore-microtubule attachment defects, known to be BubR1-dependent in mitosis (*13*), might also hinder meiotic progression. To address this possibility, we investigated two readouts of kinetochore-microtubule attachment status: Mad2, which localizes to unattached kinetochores (*14*); and the presence of cold-stable microtubules, because microtubules are unstable at 4°C unless attached to kinetochores (*13*). At 4 hours after GVBD, kinetochore-microtubule attachments have not yet formed in control oocytes (*15*), which consequently exhibit strong Mad2 staining (fig. S2B) and virtually no cold-stable microtubules (Fig. 4D). By 8 hours after GVBD, when kinetochores become fully attached, chromosomes are well aligned, Mad2 becomes undetectable (Fig. 4A and fig. S2C), and a metaphase I spindle persists after cold treatment (Fig. 4E). In stark contrast, by 8 hours after GVBD in BubR1-depleted oocytes, chromosomes are misaligned, remain strongly positive for Mad2 (Fig. 4, B and C), and have very few cold-stable microtubules (Fig. 4F). Kinetochore-microtubule attachment defects are not a consequence of the Cdc20/securin imbalance brought about by BubR1 depletion because they persist when securin expression is restrained or Cdc20 is coexpressed in BubR1-depleted oocytes (fig. S9). Thus, microtubule attachments form less efficiently after BubR1 depletion and likely explain previous observations of chromosome alignment defects in MII oocytes from BubR1-deficient mutant mice (*16*).

We show here that BubR1 sustains Cdh1 levels in prophase I and prometaphase I before inhibiting APC-Cdc20 in late MI. Cdh1 is also required for sustaining BubR1 levels, revealing a codependency between BubR1 and Cdh1 that could be relevant to the mechanism by which BubR1 stabilizes Cdh1 (fig. S10). In prophase I, BubR1-dependent Cdh1 stabilization is important for preventing unscheduled reentry into MI. After GVBD, BubR1 promotes prometaphase I progression by preventing indiscriminate securin accumulation and by contributing to the establishment of kinetochore-microtubule attachments. As part of its SAC role, BubR1 then modulates the metaphase I–to–anaphase I transition. BubR1's Cdh1-directed role appears to predominate as

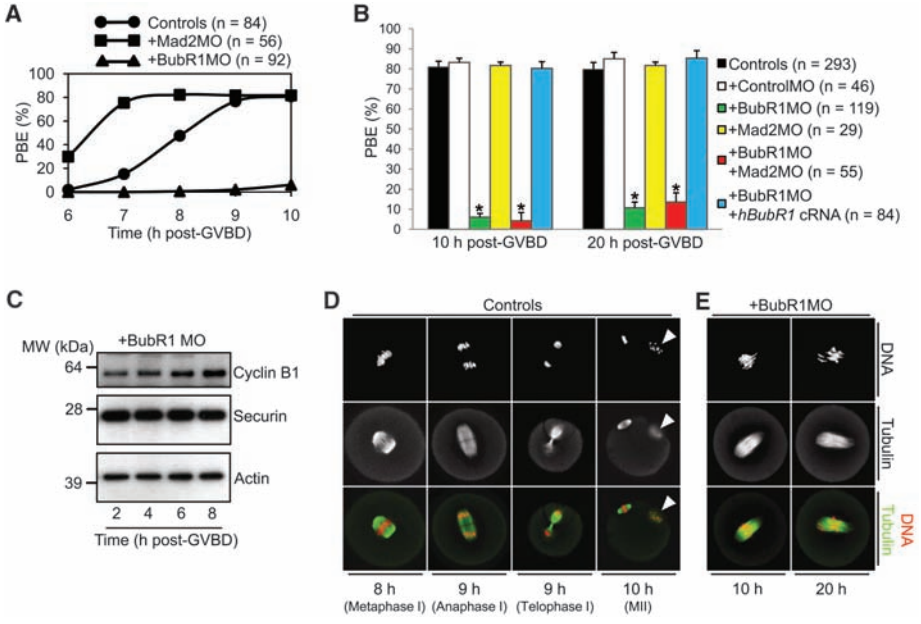

Fig. 2. BubR1 depletion induces a prometaphase I arrest. (**A**) Timeline of PBE for uninjected controls, Mad2-depleted, and BubR1-depleted oocytes. Oocytes were scored for the presence of polar bodies at 6, 7, 8, 9, and 10 hours after GVBD. Note the contrasting effects of Mad2 and BubR1 depletion on PBE. (**B**) PBE is inhibited after BubR1 depletion. PBE rates were determined at 10 and 20 hours after GVBD. Prometaphase I arrest is robust after BubR1 depletion so that PBE increases only modestly (from 6% to 11%) during an additional 10 hours of culture (from 10 to 20 hours after GVBD). Furthermore, codepletion of Mad2 does not restore PBE rates, indicating that MI arrest is not SAC-mediated. Error bars, mean + SEM; $N \geq 3$ experiments. Asterisks denote a significant difference from uninjected controls ($P < 0.0001$; Student's t test). (**C**) Samples (50 oocytes) of BubR1-depleted oocytes at 2, 4, 6, and 8 hours after GVBD were blotted for cyclin B1, securin, and actin. (**D** and **E**) Control and BubR1-depleted oocytes were immunostained for tubulin and DNA at the times after GVBD indicated in the figure ($N \geq 15$ oocytes per time point). By 10 hours after GVBD in controls, a polar body (white arrowhead) with associated chromosomes is present.

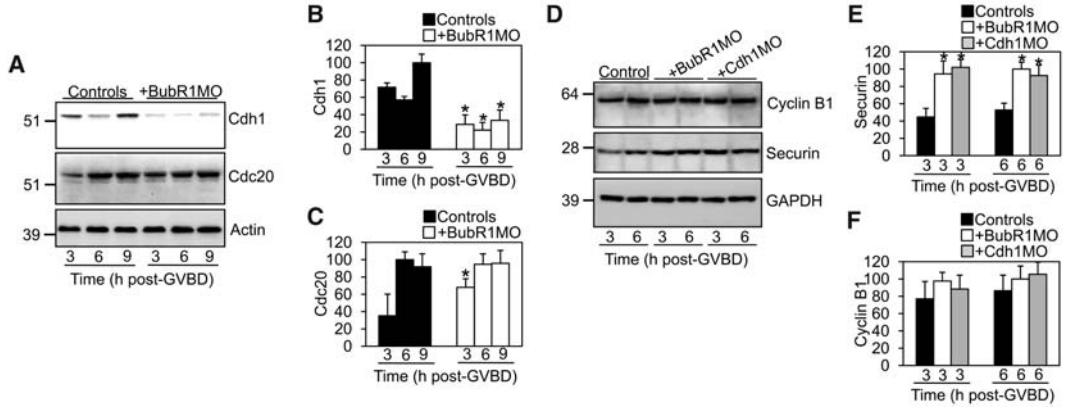

Fig. 3. (**A** to **C**) Cdh1 is reduced after BubR1 depletion. Samples (30 oocytes) of BubR1-depleted oocytes were immunoblotted along with uninjected controls at 3, 6, and 9 hours after GVBD for Cdh1, Cdc20, and actin (A). Band intensities of (B) Cdh1 and (C) Cdc20 on blots were quantified and normalized to values found in controls. (**D** to **F**) Securin is preferentially stabilized after either BubR1 or Cdh1 depletion. Samples (30 oocytes) of BubR1-depleted and Cdh1-depleted oocytes were immunoblotted along with uninjected controls at 3 and 6 hours after GVBD for securin, cyclin B1, and GAPDH (D). Band intensities of (E) securin and (F) cyclin B1 on blots were quantified and normalized to values found in controls. Error bars, mean + SEM; $N = 3$ experiments. Asterisks [(B), (C), and (E)] denote a significant difference from uninjected controls ($P < 0.0001$; Student's t test).

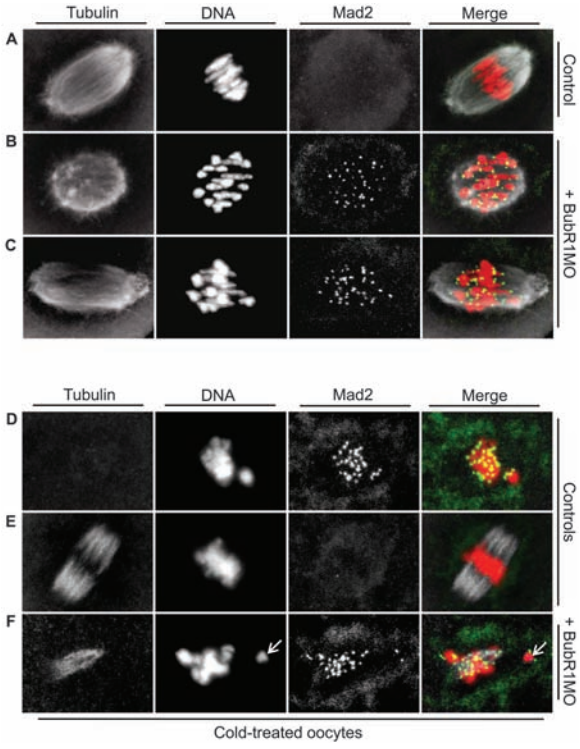

Fig. 4. BubR1 depletion impairs kinetochore-microtubule attachments. (**A** to **C**) At 8 hours after GVBD, control oocytes (A) and BubR1-depleted oocytes [(B) and (C)] were immunostained for tubulin, DNA, and Mad2. (**D** to **F**) Control oocytes were cold-treated (*9*) and immunostained at 4 (D) and 8 (E) hours after GVBD. Note the change in spindle morphology after cold treatment [compare (A) and (E)]. BubR1-depleted oocytes were cold-treated and immunostained at 8 hours after GVBD (F) ($N \geq 20$ oocytes per group). Chromosomes are extended, although kinetochore-microtubule attachments are lacking [(B) and (C)], implicating direct contacts between microtubules and chromatin as demonstrated previously (*15*). Conversely, chromosomes become compacted when microtubules are lacking (F, white arrow).

BubR1-depleted oocytes experience MI arrest while BubR1 overexpression accelerates MI (fig. S4D).

These data uncover a contrast between somatic cells and oocytes; during APC-Cdh1–dominated prometaphase I in oocytes, BubR1 promotes M-phase progression by stabilizing Cdh1, whereas in mitotic prometaphase, where APC-Cdc20 predominates, BubR1 delays anaphase onset by inhibiting APC-Cdc20. Moreover, cyclin B1 is the APC substrate that is preferentially regulated by BubR1 during mitosis (*12*), whereas during MI, it is securin. BubR1 deficiency could have grave consequences for fertility by reducing the prophase I–arrested oocyte reservoir and compromising the yield of fertilizable eggs.

References and Notes

1. J. Peters, *Nat. Rev. Mol. Cell Biol.* **7**, 644 (2006).
2. P. Marangos, J. Carroll, *Nat. Cell Biol.* **10**, 445 (2008).
3. A. Reis, H. Chang, M. Levasseur, K. Jones, *Nat. Cell Biol.* **8**, 539 (2006).
4. A. Reis *et al.*, *Nat. Cell Biol.* **9**, 1192 (2007).
5. M. Herbert *et al.*, *Nat. Cell Biol.* **5**, 1023 (2003).
6. A. Musacchio, E. D. Salmon, *Nat. Rev. Mol. Cell Biol.* **8**, 379 (2007).
7. H. Homer *et al.*, *Genes Dev.* **19**, 202 (2005).
8. B. E. McGuinness *et al.*, *Curr. Biol.* **19**, 369 (2009).
9. Materials and methods are available as supporting material on *Science* Online.
10. P. Cheslock, B. Kemp, R. Boumil, D. Dawson, *Nat. Genet.* **37**, 756 (2005).
11. N. Malmanche *et al.*, *Curr. Biol.* **17**, 1489 (2007).
12. K. B. Jeganathan, L. Malureanu, J. M. van Deursen, *Nature* **438**, 1036 (2005).
13. M. Lampson, T. Kapoor, *Nat. Cell Biol.* **7**, 93 (2005).
14. J. C. Waters, R. H. Chen, A. W. Murray, E. D. Salmon, *J. Cell Biol.* **141**, 1181 (1998).
15. S. Brunet *et al.*, *J. Cell Biol.* **146**, 1 (1999).
16. D. Baker *et al.*, *Nat. Genet.* **36**, 744 (2004).
17. This work was supported by a Wellcome Trust Clinical Fellowship (082587/Z/07/Z) to H.H. J.C. is funded by a Medical Research Council grant. We thank S. Taylor, W. Earnshaw, and K. Wassmann for reagents.

Supporting Online Material

www.sciencemag.org/cgi/content/full/326/5955/991/DC1
Materials and Methods
Figs. S1 to S11
References

22 April 2009; accepted 24 September 2009
10.1126/science.1175326

Two Chemoreceptors Mediate Developmental Effects of Dauer Pheromone in *C. elegans*

Kyuhyung Kim,[1] Koji Sato,[2] Mayumi Shibuya,[1] Danna M. Zeiger,[1] Rebecca A. Butcher,[3] Justin R. Ragains,[3] Jon Clardy,[3] Kazushige Touhara,[2] Piali Sengupta[1]*

Intraspecific chemical communication is mediated by signals called pheromones. *Caenorhabditis elegans* secretes a mixture of small molecules (collectively termed dauer pheromone) that regulates entry into the alternate dauer larval stage and also modulates adult behavior via as yet unknown receptors. Here, we identify two heterotrimeric GTP-binding protein (G protein)–coupled receptors (GPCRs) that mediate dauer formation in response to a subset of dauer pheromone components. The SRBC-64 and SRBC-66 GPCRs are members of the large *Caenorhabditis*-specific SRBC subfamily and are expressed in the ASK chemosensory neurons, which are required for pheromone-induced dauer formation. Expression of both, but not each receptor alone, confers pheromone-mediated effects on heterologous cells. Identification of dauer pheromone receptors will allow a better understanding of the signaling cascades that transduce the context-dependent effects of ecologically important chemical signals.

Pheromones are molecules secreted by an individual that induce behavioral or developmental changes in other animals of the same species (*1*). Pheromone signals can trigger long-term changes in development or physiology (primer effects) by modulating endocrine signaling and gene expression, or short-term changes in behaviors (releaser effects) via acute effects on neuronal responses (*2*). The mechanisms by which the same molecule (or molecules) can elicit these markedly distinct effects are not well understood. The nematode *C. elegans* secretes a complex mixture of chemicals that are collectively termed dauer pheromone. Dauer pheromone concentrations are assessed before the first larval molt and regulate the decision either to proceed through the reproductive cycle or to enter into the alternate, developmentally arrested dauer developmental stage (*3*, *4*). Dauer pheromone also modulates adult behaviors (*5*, *6*), indicating that it can evoke both primer and releaser effects in *C. elegans*. The active components of dauer pheromone have recently been shown to be structurally related derivatives of the dideoxysugar ascarylose (*7*–*9*), including the ascarosides C6, C9, C7, and C3 (these molecules are referred to based on the numbers of carbons in their side chains) (fig. S1). However, pheromone receptors are as yet unidentified.

In the course of searching for mutants that exhibit altered responses to dauer pheromone (*10*), we found that mutations in the predicted GTP-binding protein (G protein)–coupled receptor (GPCR) gene *srbc-64* resulted in defects in dauer formation. Loss-of-function mutations in both *srbc-64* and the closely related *srbc-66* gene (fig. S2) (*11*) resulted in similar strong defects in the ability to form dauers in response to C6, C9, and C7, with weaker defects in response to C3 (Fig. 1, A to D). These defects could be rescued upon expression of wild-type

[1]Department of Biology and National Center for Behavioral Genomics, Brandeis University, Waltham, MA 02454, USA. [2]Department of Integrated Biosciences, University of Tokyo, Chiba 277-8562, Japan. [3]Department of Biological Chemistry and Molecular Pharmacology, Harvard Medical School, Boston, MA 02115, USA.

*To whom correspondence should be addressed. E-mail: sengupta@brandeis.edu

A Spindle Assembly Checkpoint Protein Functions in Prophase I Arrest and Prometaphase Progression

Hayden Homer, Liming Gui and John Carroll

Science **326** (5955), 991-994.
DOI: 10.1126/science.1175326

BubR1 Broadens Its Remit

During mitosis in mammalian somatic cells, BubR1 is indispensable for spindle assembly checkpoint signaling and for establishing contacts between chromosomes and spindle microtubules. **Homer *et al.*** (p. 991) found that in mouse oocytes during meiosis I, BubR1 was not only required to sustain prophase I arrest but also for promoting the completion of meiosis I. Both effects converge on the Cdh1 coactivator of the multimeric ubiquitin ligase, known as the anaphase-promoting complex, and both functions are required for the production of fertilizable eggs.